IMA Conference on Mathematics of Robotics
9 – 11 September 2015, St Anne's College, University of Oxford

A Mobile Homeostat with Three Degrees of Freedom

By Steve Battle

Computer Science & Creative Technologies, University of the West of England, Bristol, UK

Abstract

In the foundational cybernetics text, *Design for a Brain*, W. Ross Ashby introduces an adaptive system called the *homeostat*, and speculates about the possibility of creating a mobile homeostat "with its critical states set so that it seeks situations of high illumination." Simulations demonstrate the viability of using the classic homeostat architecture to control a mobile robot demonstrating *ultrastability* in adapting to an environment where the goal is to stay within range of a single source of illumination. This paper explores a novel physical embodiment of Ashby's classic homeostat in a mobile robot with three degrees of freedom (2 translational, 1 rotational). The hypothesis, borne out by tests, is that the topological configuration of the robot as determined by simulation, will carry over into the physical robot.

1. Introduction

Ashby's homeostat was described by Strehl (1955) as "the most remarkable and inexplicable machine which has yet been constructed." Completed in March 1948, the homeostat comprised four identical electro-mechanical, analogue computers identified by the colours red, green, blue and yellow. Ashby (1948) described his machine thus: each unit supports a suspended magnet with a read-out needle that could be deflected by currents in the four coils beneath it. These currents flow from the other three units and also within a feedback loop from each unit back to itself. The effect of one unit upon another can be individually configured. A configuration is unstable if some or all of the read-out needles get stuck at their physical limits for any appreciable length of time. There are however, stable solutions where the needles freely come to rest or exhibit dynamic stability in a steady oscillation.

Ashby (1952) defines the second-order differential equation of the homeostat in the appendices of *Design for a Brain* which is reproduced in Equation 1.1 below, for n units ($1 \leq i \leq n$). The variables x_i represent the output of each homeostat unit. The signed weights $a_{i,k}$ are applied to the input to unit i from unit k, while the factor h adjusts their effect on the read-out needle via the coils. The factor j counteracts this effect, representing drag on the movement of the read-out needle in response to the magnetic field of the coils.

$$\ddot{x_i} = h \sum_{k=1}^{n} a_{i,k} x_k - j\dot{x_i} \tag{1.1}$$

For simplicity, the constants h and j may both be set to 1, as verified in simulation.

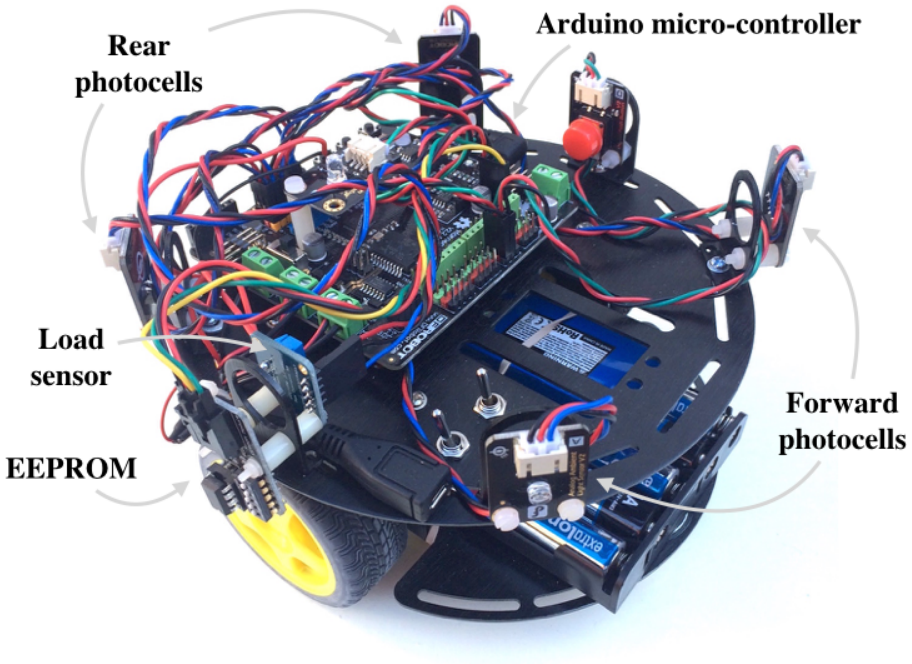

FIGURE 1. Construction of the mobile homeostat.

2. Essential variables

The innovation of the homeostat is Ashby's double feedback loop. This models how an organism detects conditions that threaten its survival. A subset of homeostat units are characterized as *essential* variables with lower and upper bounds. When these bounds are exceeded the homeostat undergoes a random reconfiguration, effectively transforming itself into a new machine Boden (2006). The homeostat thus performs a random search for a combination of weights that provide a stable configuration both internally and in response to its environment, Ashby (1948). This is adaptation through *ultrastability*.

In the context of the *mobile* homeostat the primary essential variable is the level of illumination by the light source as set out by Ashby. However, even the individual units controlling the motors must be treated as essential variables to prevent them saturating at their limits as a consequence of runaway positive feedback. The robot described here moves freely in a 2 dimensional plane. Having differential steering it has 2 translational, and 1 rotational degrees of freedom. This extends earlier work, Franchi (2013), that explores a mobile homeostat with 1 degree of freedom.

3. Robot construction

Instead of read-out needles we connect the homeostat outputs to the motors of a physical robot, illustrated in Figure 1. Simulations show that a two-unit homeostat is sufficient to control a robot with 2 degrees of freedom, Battle (2014). Furthermore, Ashby's *Law of Requisite Variety* suggests that a control system need be no more complex that the environment it has to control. Further simulations demonstrate that a homeostat with reduced connectivity, breaking all internal connections between the two units, is capable of controlling such a robot. Communication between the two units is still possible, but any information must pass indirectly via the environment. This then, is the initial basis

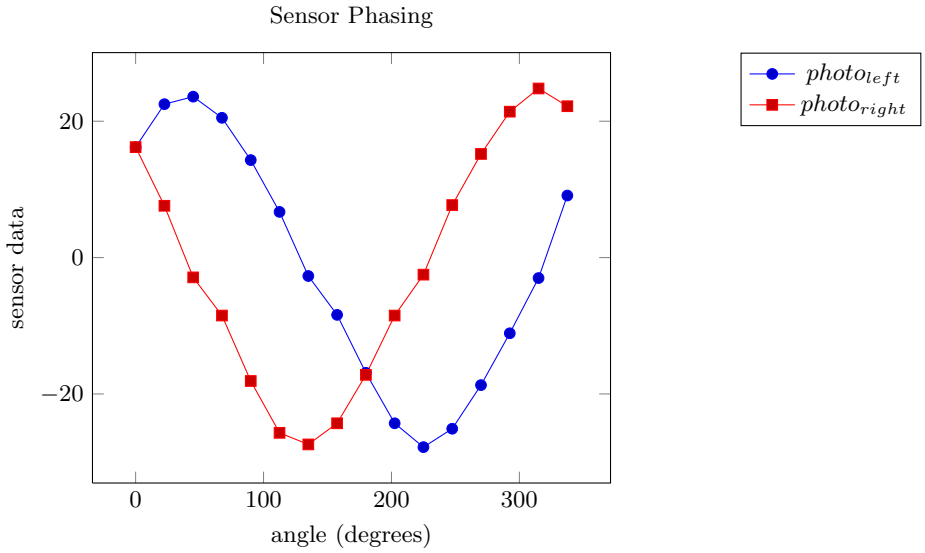

FIGURE 2. Data for the left and right $front - rear$ photocell assemblies as the robot is rotated at a fixed distance from the light source.

of the physical robot configuration. While it is expected that the physical robot and environment will behave differently to the simulation, the hypothesis is that the broad topological configuration of the robot (number of units, connectivity) as determined by simulation, will carry over into the physical robot. If this hypothesis is true then there should exist a stable solution for the 2-unit, internally disjoint mobile homeostat.

The mobile homeostat is a simple robot platform designed to demonstrate Ashby's principle of *ultrastability* applied to a robot. Its movement need not be especially accurate so two DC motors are sufficient to provide differential steering. The motor output from the homeostat is bounded within the range [-1,1] with +1 corresponding to full-speed forward and -1 corresponding to full-reverse. The only other object in the universe of the robot is the central light source. If the robot collides with the light source itself, as detected by a load (current) sensor on the motor driver, then a simple *avoidance* strategy reverses the robot for one second before triggering a new random configuration. The robot also has a *recovery* behaviour that returns the robot to a predefined distance from, and orientation with, the light source. This behaviour is invoked when the robot strays too far from the light, which again is accompanied by a random reconfiguration.

The homeostat implementation solves Equation 1.1 using Euler's forward method which provides a rapid iterative approach that lends itself to solving differential equations in real-time. Ashby suggested that essential variables should not be checked continuously but perhaps every 3 seconds or so, the trial period used in these experiments. When a given configuration survives a full minute (20 trial periods) then the solution is deemed to be stable. The robot has a small EEPROM to which it can record stable configurations and log its state variables for analysis.

4. Phased sensors

Four photocells provide the robot with information about its position relative to the single light source. These photocells are spaced at 90° around the outside of the chassis.

If we take the front of the robot to be at 0° then the photocells are mounted at 45°, 135°, 225°, and 315°, such that the two forward facing photocells are mounted 45° either side of centre. The amount of light energy falling on a surface is proportional to the cosine of the angle of incidence. Photocells facing away from the light source receive little or no energy. Therefore, if the robot is rotated the signal from each sensor is a half-wave rectified sinewave. The photocells on opposite sides of the robot are then paired up such that the forward facing photocells provide the positive component of the signal, while rear facing photocells provide the negative component. The output from the rear facing photocells may be subtracted from the forward facing photocells resulting in a pair of sinewaves 90° out of phase with each other. In Figure 2 the robot was held at a fixed distance from the light source and the combined forward/rear facing outputs are plotted against each other as the robot is rotated through 360°.

5. Brightness constancy

The key to providing input to the homeostat is to eliminate unnecessary variability. As light intensity falls with distance according to the inverse square law, the amplitude of the raw photocell data varies as a function of distance as illustrated in Figure 3. The variety of the input can be reduced by eliminating this dependency. The normalized input signal will vary only as a function of the angle of incidence. This *brightness constancy*, irrespective of distance, is common in nature allowing visual objects to be perceived as having the same brightness under different illumination conditions.

In order to recover the angular data, the magnitudes of the combined photocell signals must be discarded. Because of the placement of the photocells, the ratio between the left and right photocell assemblies is the tangent ratio so the angle θ can be recovered by taking the arctangent (atan2) based on the simple trigonometric relationship, below.

$$tan(\theta) = \frac{photo_{left}}{photo_{right}} \tag{5.1}$$

The normalized inputs for the left and right-hand photocell assemblies can then be obtained using the trigonometric equations for the unit circle.

$$norm_{left} = sin(\theta) \tag{5.2}$$

$$norm_{right} = cos(\theta) \tag{5.3}$$

Figure 3 contrasts the raw signal from the photocells with the normalized input. The robot is held directly facing the light source so that the amount of light falling on the left and right-hand photocells is equal. The robot is moved between 50cm to 450cm from the light source so that the decrease in intensity due to the inverse square law can be observed at the photcells. For comparison, the normalized value for the left-hand input is plotted and this is seen to be relatively constant reflecting the constant angle. The normalized output for the right-hand side is almost identical, θ is determined as above.

$$sin(\theta) \approx cos(\theta) \approx 0.70 \pm 0.005 \tag{5.4}$$

6. Illumination level

A reliable estimate of the overall level of illumination is required, being the primary essential variable in the environment. The data from the photocells must be combined to provide an esitmate of illumination that is independent of the angle of the robot to the

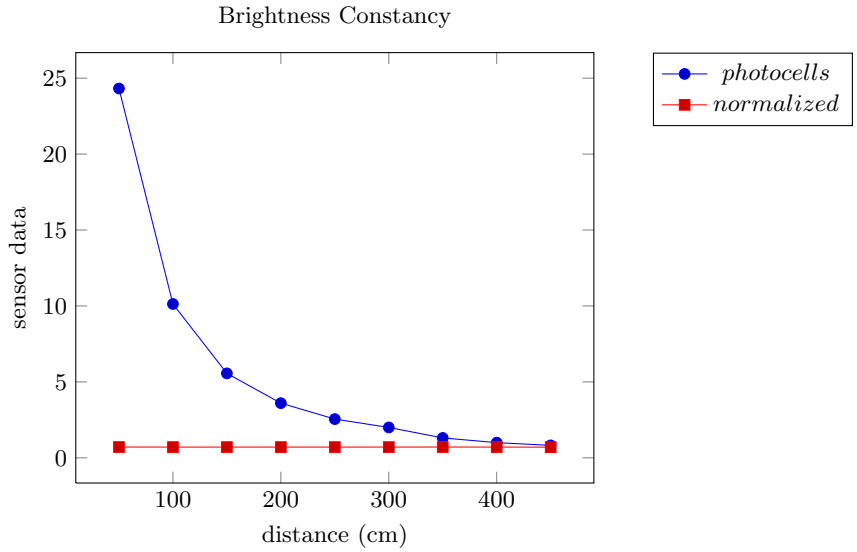

FIGURE 3. Photocell data is plotted for the left-hand input, falling with distance in accordance with the inverse square law. The normalized left-hand input is plotted for comparison. The robot is held directly facing the light source so the data for the right-hand side are almost identical.

light source. The inverse square law states that the light intensity falls proportionally to the square of the distance from the light source as in Equation 6.1. However, for a non-perpendicular angle of incidence Lambert's cosine law may be used instead to model the light falling on a given photocell. The light energy E falling on the left and right-hand photocell assemblies is modelled in Equations 6.2 & 6.3 below where I is the intensity of the light source at the origin and d is the distance. As the photocells are oriented at 90° to each other, sine and cosine are used in the expression of Lambert's law.

$$E = \frac{I}{d^2} \tag{6.1}$$

$$photo_{left} = \frac{I\sin(\theta)}{d^2} \tag{6.2}$$

$$photo_{right} = \frac{I\cos(\theta)}{d^2} \tag{6.3}$$

The Pythagorean theorem is used to combine the sensor data into a single estimate for E. Substituting E for r in Equation 6.4 below we obtain Equations 6.5 and finally Equation 6.6 expressed in terms of the raw photocell data.

$$r^2 = (r\sin(\theta))^2 + (r\cos(\theta))^2 \tag{6.4}$$

$$\left(\frac{I}{d^2}\right)^2 = \left(\frac{I\sin(\theta)}{d^2}\right)^2 + \left(\frac{I\cos(\theta)}{d^2}\right)^2 \tag{6.5}$$

$$\left(\frac{I}{d^2}\right)^2 = photo_{left}^2 + photo_{right}^2 \tag{6.6}$$

We thus obtain an estimate of the overall light intensity independent of its angle with

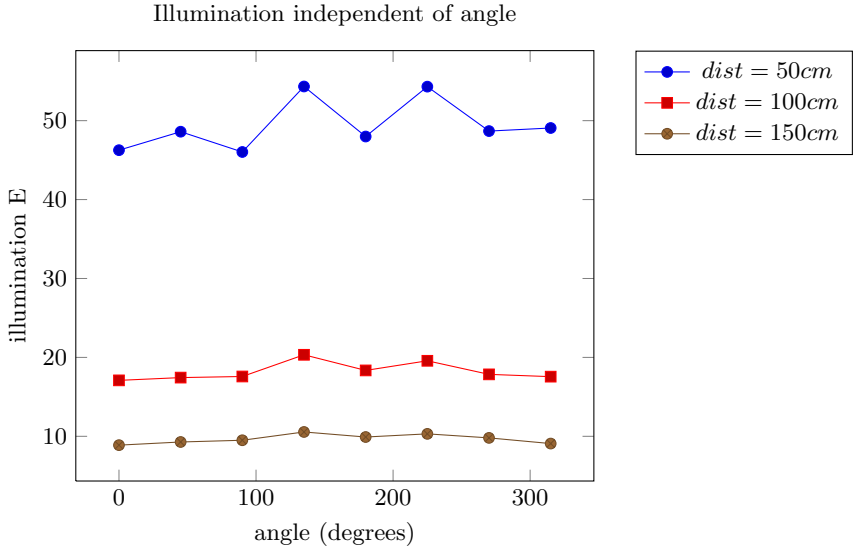

FIGURE 4. Illumination E derived from a pythagorean combination of photocell sensor data. The robot is held at distances of 50cm, 100cm, 150cm and rotated through 360°.

respect to the light source. This is tested on the robot in Figure 4 where the light intensity is calculated while the robot is held at a fixed position and rotated through 360°. It may be seen that the error is reduced with increasing distance as the light source better approximates a point source of light.

7. Analysis

The mobile homeostat finds many stable solutions, many of which may be described as *degenerate* as they simply involve the robot spinning on the spot. Staying still is often the easiest way to maintain a constant level of illumination. However, we're more interested in goal-seeking, dynamic stability. Here we examine a so-called *orbital* solution where the robot maintains dynamic stability for at least one minute.

Figure 5 spans 30 seconds of telemetry from the robot in orbit around the light source, with each orbit lasting approximately 6.7 seconds; the cycle time of the oscillations seen in the plot. The 5 traces represent 2 state-variables with 3 additional inputs. The two solid lines are the left/right motor outputs. Observe that both motor traces are less than zero which means that the robot is actually driving in reverse. The left-hand motor output has a consistently greater magnitude than the right-hand side resulting in an anticlockwise circular motion. The dashed lines are the normalized inputs from the left/right photocell assemblies. The photocell data, normalized for brightness constancy, is positive on the right-hand side and negative on the left-hand side indicating that the light-source lies to the right of the robot. The photocell data are combined in the green trace which represents the derived illumination level, E, independent of angle. This never falls below the minimum illumination level (0.1) at which point the weights would be randomized.

The mobile homeostat is described as a *machine with input*, Ashby (1956). The homeostat Equation 1.1 is adapted to accept $n+p$ weights for each of n units where there are p additional input parameters. These define an $(n+p)\times n$ matrix. The mobile homeostat has $n = 2$ units and $p = 3$ additional parameters. The matrix of Equation 7.1, below represents the weight matrix for an orbital behaviour discovered by the robot. Each col-

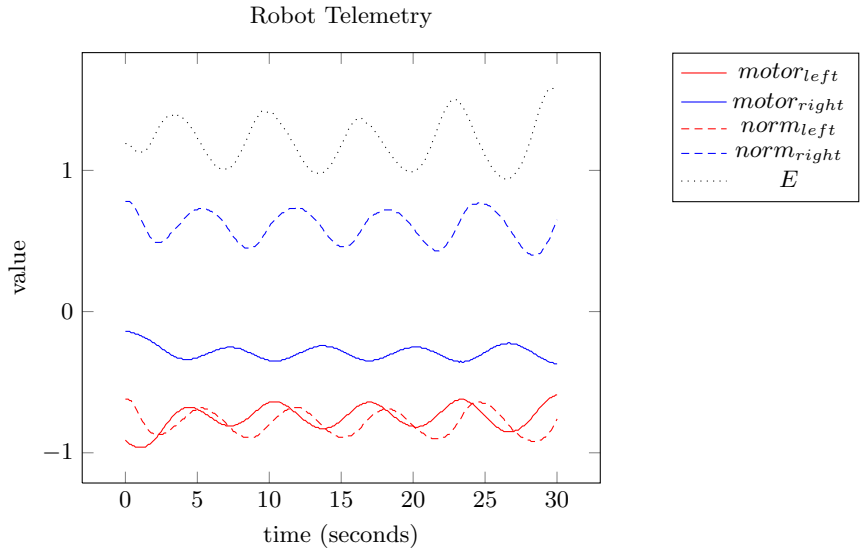

FIGURE 5. Telemetry from the mobile homeostat over a 30sec window showing two state variables representing motor outputs, and three sensor inputs derived from the photocells.

umn defines a set of input weights for one unit. The 0 entries are the severed connections that cannot be changed automatically. The values of -0.7 represent an arbitrary level of feedback that is also not under automatic control. Similarly the 1 entries which enable the thresholded illumination signal at full strength also cannot be changed because this is an essential variable in the environment that cannot be ignored. The outputs from each unit and the parameters are marshalled together into a 1D matrix x defined in Equation 7.2 that is multiplied by the weight matrix giving e.

$$e = x \times \begin{pmatrix} -0.7 & 0 \\ 0 & -0.7 \\ 0.10 & 0.34 \\ -0.72 & 0.10 \\ 1.0 & 1.0 \end{pmatrix} \tag{7.1}$$

$$x = (motor_{left},\ motor_{right},\ norm_{left},\ norm_{right},\ min \not< E)) \tag{7.2}$$

One analysis that can be performed is to explore where *idealized* stable solutions exist, or don't exist, for this weight matrix. The homeostat Equation 1.1 is a second-order system, where the output from the weight multiplication represents the error. To achieve a (static) stable solution the error e must be zero and the 2nd order term $\ddot{x_i}$ would then tend to zero. This is clearer in Ashby's reformulation of the homeostat as a first-order system in Equation 7.3 which holds over longer timescales, showing the homeostat to be state-determined and linear.

$$\dot{x_i} = \sum_{k=1}^{n} a_{i,k} x_k \tag{7.3}$$

We solve the linear equations represented by the matrix assuming an error of zero; e is the zero matrix. The machine with input is not represented by a square matrix so the problem is underspecified and there are infinitely many solutions. Given this and to

avoid the trivial solution where x equals the zero matrix, we introduce representative bounds on the solution. In the telemetry data of Figure 5 it was observed that the robot is driving in reverse, so both motor units are less than zero. The left-hand sensor input is less than zero, while the right-hand sensor input is greater than zero. This set of bounds is verified using the GNU Octave solver setting representative upper bounds of -0.1 on $motor_{left}$, $motor_{right}$ and an upper bound of 0 on $norm_{left}$, and a lower bound of 0 on $norm_{right}$. The equation solver finds one solution for x below, in Equation 7.3, verifying that at least one stable solution exists within these bounds (see Appendix).

$$x = (-1.00000,\ -0.10000,\ -0.47253,\ 0.90659) \tag{7.4}$$

For comparison, the relative positions of the robot and light source may be reversed, requiring the left-hand sensor to be positive and the right-hand sensor negative. This set of bounds has no solution corroborating the evidence that this is an unstable configuration.

8. Conclusion

The construction of the physical mobile homeostat and the fact that it finds an orbital solution validates the hypothesis that the topological configuration of the robot as determined by simulation, carries over into the physical robot. The robot itself demonstrates a number of interesting features. A surprising amount of information can be gleaned from four simple photocells supporting brightness constancy independent of distance, and illumination independent of angle. These experiments validate Ashby's thought experiment about the possibility of creating a mobile homeostat.

9. APPENDIX: GNU Octave bounded model for $ax = b$

```
a=[-0.7,0; 0,-0.7; 0.1,0.34; -0.72,0.1]'; b=[0,0]'; c=[1,2,3,4]';
lb=[-1,-1,-1,0]; ub=[-0.1,-0.1,0,1]; ctype="SS"; vartype="CCCC";
s=-1; param.msglev=1; param.itlim=100;
[xmin, fmin, status, extra] = ...
   glpk (c, a, b, lb, ub, ctype, vartype, s, param);
xmin
# ax=b is unsolvable after reversal of the sensors
lb=[-1,-1,0,-1]; ub=[-0.1,-0.1,1,0];
[xmin, fmin, status, extra] = ...
   glpk (c, a, b, lb, ub, ctype, vartype, s, param);
xmin
```

REFERENCES

Ashby, W. R. 1948 *Design for a Brain. Electronic Engineering.* **20**, 379–383.

Ashby, W.R. 1952 *Design for a Brain.* Chapman & Hall.

Ashby, W.R. 1956 *An Introduction to Cybernetics.* Chapman & Hall, London.

Battle, S. 2014 Ashby's Mobile Homeostat. In *Artificial Life and Intelligent Agents 2014.*

Boden, M. 2006, *Mind as Machine: A History of Cognitive Science.* Clarendon Press.

Franchi, S. 2013, Homeostats for the 21st Century? Simulating Ashby Simulating the Brain, Constructivist Foundations 9(1): 93-101.

Strehl, R. 1955 *the robots are among us.* Arco Publishers.